# Regulation of autophagy-related mechanisms during bacterial infection

Xie, J.

# Chapter 2

# Chapter 2

## DRAM1 confers resistance to *Salmonella* infection

Samrah Masud*, Jiajun Xie*, Bart J.M. Grijmans, Sander van der Kooij,
Rui Zhang, Tomasz K. Prajsnar and Annemarie H. Meijer

*Autophagy Reports 2023, 2: 2242715*
* these authors contributed equally to this work and share first authorship

# ABSTRACT

DRAM1 is an infection inducible autophagy modulator, previously shown to promote autophagic and lysosomal defense responses against the intracellular pathogen *Mycobacterium marinum*. However, its possible role in other anti-bacterial autophagic mechanisms remains unknown. Recently, LC3-associated phagocytosis (LAP) has emerged as autophagy-related mechanism that targets bacteria directly in phagosomes. Our previous work established LAP as the main autophagic mechanism by which macrophages restrict growth of *Salmonella* Typhimurium in a systemically infected zebrafish host. We therefore employed this infection model to investigate the possible role of Dram1 in LAP. Morpholino knockdown or CRISPR/Cas9-mediated mutation of *dram1* led to reduced host survival and increased bacterial burden during *S*. Typhimurium infection. In contrast, overexpression of *dram1* by mRNA injection curtailed *Salmonella* replication and reduced mortality of the infected host. During the early response to infection, GFP-Lc3-*Salmonella* colocalization were reduced in *dram1* knockdown or mutant embryos, and increased by *dram1* overexpression. Since LAP is known to require the activity of the phagosomal NADPH oxidase, we used a *Salmonella* biosensor strain to detect bacterial exposure to reactive oxygen species (ROS) and found that the ROS response was largely abolished with deficiency of Dram1, while it was increased with *dram1* overexpression. Corroborating these results in a mammalian model, the LC3 and ROS responses to *Salmonella* were similarly reduced or increased by knockdown or overexpression of *Dram1*, respectively, in murine RAW 264.7 macrophages. Together, these results demonstrate the host protective role of Dram1/DRAM1 during *S*. Typhimurium infection and suggest a functional link between Dram1/DRAM1 and the induction of LAP.

## Introduction

Macroautophagy/autophagy has long been known as a fundamental housekeeping process wherein dysfunctional cellular components are captured inside double membrane vesicles that fuse with lysosomes to degrade and recycle the contents (Levine and Klionsky, 2004; Mizushima, 2007). More recently, autophagy has also been recognized as an integral part of the immune system, functioning not only as a direct anti-microbial mechanism but also contributing to regulation of the immune response (Deretic et al., 2013). Autophagy can function as a non-specific bulk process or as a selective mechanism mediated by receptors that recognize molecular degradation signals like ubiquitin (Boyle and Randow, 2013). The selective autophagy of invading microbes, referred to as xenophagy, is an innate immune effector mechanism targeting invading microbes either when present inside membrane-bound compartments or when they escape into the host cytosol (Huang and Brumell, 2014). Xenophagy and other autophagy-related processes have been shown as an important mechanism for resistance to infections, but pathogens have evolved various mechanisms to subvert these defenses (Deretic et al., 2006; Huang and Brumell, 2014; Hubber et al., 2017; Mostowy, 2013; Prajsnar et al., 2021).

A hallmark of all forms of autophagy is the conjugation of autophagy related protein 8 (ATG8) family proteins, including microtubule-associated protein 1 light chain 3 (MAP1LC3, hereafter LC3), with phospholipids on the autophagosomal double membrane structures (Mizushima et al., 2004). However, LC3 can also be recruited to vesicles with a single membrane, a process named Conjugation of ATG8 to endolysosomal Single Membranes (CASM) (Durgan and Florey, 2021; Durgan et al., 2021). One example of CASM is LC3-associated phagocytosis (LAP), where LC3 is recruited to phagosomes, thereby forming LAPosomes (Martinez, 2018; Sanjuan et al., 2007; Upadhyay and Philips, 2019). In LAP, the class III phosphatidylinositol 3-kinase (PI3KC3) complex containing (run domain Beclin-1-interacting and cysteine-rich domain-containing protein (Rubicon/RUBCN) and UV radiation resistance associated protein (UVRAG)) generates and delivers phosphatidyl-inositol 3-phosphate (PI3P) onto the phagosomal membrane and interacts with ATG16L1 to initiate LC3 conjugation (Grijmans et al., 2022; Lei and Klionsky, 2022; Martinez et al., 2015). Rubicon is an essential positive regulator of LAP, but is dispensable for other forms of CASM and has a negative regulatory role in canonical autophagy (Hooper et al., 2022; Martinez et al., 2015). A hallmark of LAP is the production of reactive oxygens species (ROS) by the NADPH oxidase 2 complex (NOX2), which precedes LC3 recruitment. ROS play an

essential role in LAPosome maturation. Specifically, ROS has been shown to inactivate ATG4B, thereby inhibiting the proteolytic release of LC3 and stabilizing the LAPosome (Ligeon et al., 2021). Furthermore, production of ROS by NOX2 consumes $H^+$ and thus causes a higher pH in the phagosome, which is necessary for V-ATPase assembly: the critical regulating step that drives ATG16L1 recruitment and LC3 conjugation, not only in LAP but in all other forms of CASM (Grijmans et al., 2022; Hooper et al., 2022). Similar to xenophagy, LAP has been implicated in the host response to a wide variety of pathogens (Grijmans et al., 2022).

There are various ways in which autophagy-dependent mechanisms can be induced in response to internal and external stress factors, such as nutrient restriction, DNA damage, and microbial invaders. One factor implicated in the activation of autophagy is DNA damage regulated autophagy modulator gene 1 (*DRAM1*), which encodes a member of an evolutionary conserved family of six transmembrane proteins (Mah et al., 2012). *DRAM1* was first reported as direct target gene of the tumor suppressor protein p53 and shown to play a role in p53-mediated autophagy and apoptosis (Crighton et al., 2006). DRAM1 has been implicated in several types of cancers (Chen et al., 2018; Galavotti et al., 2013; Meng et al., 2018). Overexpression of *DRAM1* has been shown to increase basal levels of autophagosome numbers, indicating that DRAM1 can act early in the autophagy process, contributing to autophagosome formation (Mah et al., 2012). However, the DRAM1 protein predominantly localizes to lysosomes and there is also an evidence for its functions at later steps in the process, showing that DRAM1 enhances autophagic flux and promotes ATPase activity and lysosomal acidification (Geng et al., 2020; Zhang et al., 2013). DRAM1 is thought to mediate crosstalk between autophagy and apoptosis by interacting with the proapoptotic protein BAX (Guan et al., 2015). Furthermore, in an autophagy-independent manner, DRAM1 interacts with transporter proteins to promote lysosomal amino acid efflux, which activates the nutrient-sensing complex mTORC1 (Beaumatin et al., 2019). Other molecular interactions of DRAM1 that could explain its mode of action at early as well as late steps of the autophagy pathway remain to be elucidated.

In addition to DNA damage, *DRAM1* is induced by infection (Laforge et al., 2013; van der Vaart et al., 2014). In HIV-infected T-cells, DRAM1 has been shown to function downstream of p53, triggering lysosomal membrane permeabilization and cell death (Laforge et al., 2013). In contrast, we have shown that the induction of *DRAM1* in macrophages infected with *Mycobacterium tuberculosis* is independent of p53 and mediated instead by transcription factor NFκB, which functions downstream of pathogen

recognition by Toll-like receptor (TLR) signaling (van der Vaart et al., 2014). Similarly, induction of the zebrafish homologue of *DRAM1* (*dram1*) by *Mycobacterium marinum* infection relies on the TLR adaptor molecule MyD88 (van der Vaart et al., 2014). *M. marinum*-infected zebrafish embryos develop a tuberculosis-like disease and we have shown that Dram1 plays a host protective role in this model (Meijer and van der Vaart, 2014; van der Vaart et al., 2014; Zhang et al., 2020). Failing to contain the intracellular infection, macrophages in *dram1-/-* zebrafish succumbed to pyroptotic cell death (Zhang et al., 2020). Likewise, *Dram1* knockdown in murine RAW 264.7 macrophages led to increased cell death of infected macrophages and increased *M. marinum* growth. Both in zebrafish and in murine RAW 264.7 macrophages, we found that deficiency of Dram1/DRAM1 not only reduces the colocalization of Lc3/LC3 with *M. marinum* but also markedly reduces the acidification of *M. marinum*-containing vesicles (Meijer and van der Vaart, 2014).

Based on its host-protective role in *M. marinum* infection, we hypothesize that Dram1/DRAM1 also confers protection against other intracellular pathogens targeted by autophagic processes, not limited to xenophagy but also including LAP. Therefore, in the present study we sought to investigate the role of Dram1/DRAM1 in host defense against *Salmonella enterica* serovar Typhimurium (*S*. Typhimurium). A zebrafish model for *S.* Typhimurium infection has previously been established and *dram1* expression is inducible following intravenous injection of the pathogen in this model (Stockhammer et al., 2010; Van Der Sar et al., 2003). In our recent work, we have shown that LAP is the main autophagic process targeting *S.* Typhimurium following phagocytosis of the pathogen by macrophages in the zebrafish host (Masud et al., 2019a). Inhibition of LAP, by knockdown of factors specific for this process (Rubicon and NADPH oxidase), impaired host resistance (Masud et al., 2019a; Masud et al., 2019b). Here, we demonstrate that Dram1/DRAM1 is required for host resistance to *S.* Typhimurium infection and promotes the LAP-associated ROS response to this pathogen both in the zebrafish host and in mammalian macrophages.

## Results

### Knockdown and overexpression of *dram1* indicates its function in zebrafish host defense against *Salmonella* infection

In order to investigate the role of Dram1 during *Salmonella* infections, we modulated levels of *dram1* either by knockdown using a splice blocking morpholino or by overexpression through mRNA injection at the 1-2-cell stage of zebrafish embryos. We challenged the host at 2 days post fertilization (2 dpf) with *S*. Typhimurium by intravenous injection and recorded progression of the resulting infection by survival curves and colony-forming unit (CFU) determination **(Figure 1A)**. We found that *dram1* knockdown resulted in hypersusceptibility to *Salmonella* infection, where at 48 hours post infection (hpi) nearly 74 % of hosts succumbed to *S*. Typhimurium infection in significant contrast to 54 % of mortality in control hosts **(Figure 1B)**. Moreover, only 4 % of *dram1*-deprived hosts were alive at 72 hpi compared to 29 % of the control group **(Figure 1B)**. Additionally, under knockdown conditions of *dram1*, infected hosts contained significantly higher *S*. Typhimurium bacterial counts at 24 hpi **(Figure 1C)**. Conversely, the overexpression of *dram1* by mRNA injection resulted in higher survival rates **(Figure 1B)** and lower numbers of *S.* Typhimurium bacteria at 24 hpi **(Figure 1C)**. These results indicate that Dram1 restricts *Salmonella* infection in the host.

### Dram1 is required for the Lc3 response of the zebrafish host that targets *Salmonella* phagocytosed by macrophages

We have previously shown that the autophagy response of macrophages towards *Salmonella* in our model occurs mainly as LAP (Masud et al., 2019a). To study whether Dram1 contributes to the Lc3 targeting of *Salmonella*, we injected *dram1* morpholino into embryos of the *Tg(CMV:GFP-maplc3b1)* line (hereafter referred to as GFP-Lc3) and infected these with *mCherry*-expressing *S*. Typhimurium **(Figure 2A)**. We observed that GFP-Lc3 colocalization with *Salmonella* cells were significantly Dram1 dependent, since morpholino knockdown resulted in more than two-fold reduction of GFP-Lc3-positive infected phagocytes **(Figure 2B,C)**. Thus, the increased susceptibility of *dram1* knockdown embryos **(Figure 1)** is associated with diminished levels of Lc3-*Salmonella* colocalization. Next, we investigated if the positive effect of mRNA-mediated *dram1* overexpression on restricting infection **(Figure 1)** is accompanied by an increased Lc3 response towards the

pathogen. Indeed, infection of control and *dram1* overexpressing GFP-Lc3 embryos showed a significant increase of GFP-Lc3 colocalization with *S.* Typhimurium bacterial cells in the overexpression group **(Figure 2B,C)**. These results lead us to propose that Dram1 promotes the LAP response during *Salmonella* infections, resulting in a more effective host defense.

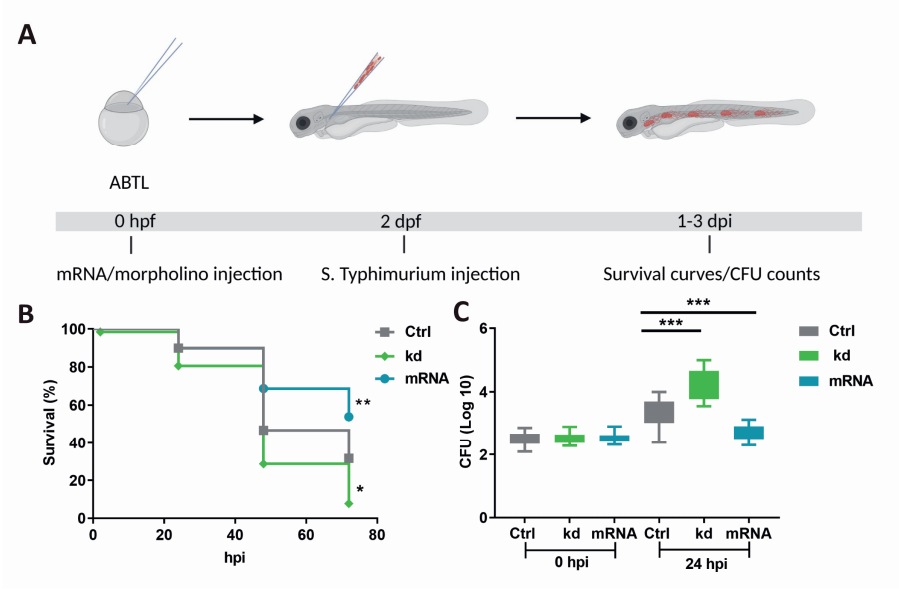


**Figure 1: Dram1 is required for effective host defense during *Salmonella* infection in zebrafish.** (**A**) Workflow of experiments followed in B-C along with the timeline of developing embryos. (**B**) Survival curves of embryos with *S.* Typhimurium infection expressing different levels of *dram1*. Control embryos were compared to *dram1* knockdown (kd) and overexpression (mRNA) groups, and survival curves show the data from three independent experiments (n=150 embryos/group). (**C**) CFU counts for infected embryo groups in B. The log transformed CFU data from three independent experiments are shown with the geometric mean per time point (n=15 embryos/group). Error bars represent SD. Statistical significance of survival curves data is assessed by Cox proportional hazards model with log rank test, and pairwise comparison with Dunnett correction. Statistical significance of CFU counts data is analyzed by one-way ANOVA and pairwise comparison with Dunnett correction. (*p<0.05; **p<0.01; ***p<0.001).

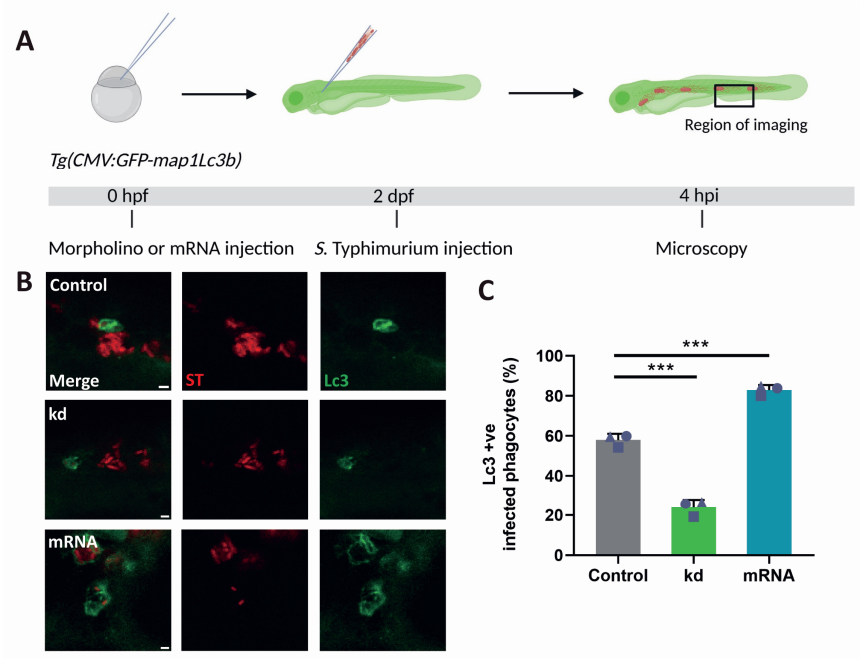


**Figure 2: Dram1 promotes GFP-Lc3 colocalization with *Salmonella* in macrophages of the zebrafish.** (**A**) Workflow and timeline of experiments in B-C. (**B**) Representative confocal micrographs of *Tg(CMV:GFP-maplc3b1)* embryos from *dram1* knockdown, overexpression and control groups infected with *mCherry*-expressing *S*. Typhimurium (ST) at 4 hpi. Scale bar = 5µm (**C**) Quantification of GFP-Lc3-*Salmonella* colocalization at 4 hpi. Error bars represent SD. The bar graph shows the data from three independent experiments, where the mean of each replicate is indicated with a different symbol (n= 15 embryos/group). Statistical significance is analyzed by one-way ANOVA and pairwise comparison with Dunnett correction. (***p<0.001).

## Mutation of *dram1* in zebrafish recapitulates the infection phenotype of *dram1* morpholino-induced knockdown

In order to verify the results obtained using morpholino-mediated knockdown, we studied *S*. Typhimurium infection in a previously established *dram1* mutant line (Zhang et al., 2020). We infected *dram1*-/- and *dram1*+/+ embryos with *S*. Typhimurium **(Figure 3A)** and observed that *dram1*-/- hosts showed increased mortality during *S*. Typhimurium infection as compared to *dram1*+/+ controls **(Figure 3B)**. Bacterial growth determination confirmed the *Salmonella*-restricting role of Dram1 as significantly higher bacterial counts were retrieved from *dram1*-/- embryos at 24 hpi as compared to *dram1*+/+ embryos **(Figure 3C)**. The *dram1* mutants were subsequently tested for Lc3 targeting of *Salmonella*. We observed significantly less GFP-Lc3 colocalization

with *Salmonella* cells in *dram1-/-* embryos compared to *dram1+/+* embryos **(Figure 3D,E)**, further confirming our initial observations using morpholino knockdown. The consistent results obtained in Dram1-deficient hosts achieved by knockdown or stable mutation support the function of Dram1 in LAP-mediated host defense during *Salmonella* infections.

**Dram1 is required for the phagocyte ROS response associated with LAP in infected zebrafish**

LAP has been shown to depend strictly on NADPH oxidase and Rubicon-mediated generation of ROS (Martinez, 2018). To confirm that zebrafish macrophages mount a LAP response towards *S*. Typhimurium, we adopted a pharmacological approach where we used a chemical inhibitor, 2-(tetrahydroindazolyl) phenoxy-N-(thiadiazolyl)propanamide (TIPTP), which interferes with the interaction between NADPH oxidase and Rubicon (Kim et al., 2020). First, we verified that TIPTP did not affect *S.* Typhimurium growth **(Fig S1)**. Next, to analyze the effect of TIPTP during infection we utilized an *S.* Typhimurium ROS biosensor strain that contains a constitutively expressed *mCherry* reporter and a GFP reporter that is activated when bacterial cells are exposed to ROS (Burton et al., 2014) **(Figure 4A)**. We have previously shown that the activation of this ROS biosensor is strictly dependent on the expression of Rubicon and the NADPH oxidase component Cyba, demonstrating that this biosensor is a reliable indicator of the occurrence of LAP (Masud et al., 2019a). We found that activation of the ROS biosensor was strongly reduced in the presence of TIPTP, providing further evidence that the bacterial ROS response requires the activity of the LAP factors, NADPH oxidase and Rubicon (**Figure 4B,C**). Next, to study the link between Dram1 and the LAP response to *S.* Typhimurium, we determined the effect of Dram1 deficiency on the ROS biosensor strain **(Figure 5A)**. We observed that activation of the ROS biosensor was reduced in *dram1*-/- hosts compared to *dram1*+/+ individuals **(Figure 5B, C)**. Furthermore, overexpression of *dram1*, by means of mRNA injection (**Fig S2**), increased activation of the ROS biosensor **(Figure 5D,E)**. Together, our results demonstrate that Dram1 is required for both GFP-Lc3 recruitment and ROS generation in infected phagocytes of the zebrafish host, consistent with the proposed role of Dram1 in the LAP response to *Salmonella*.

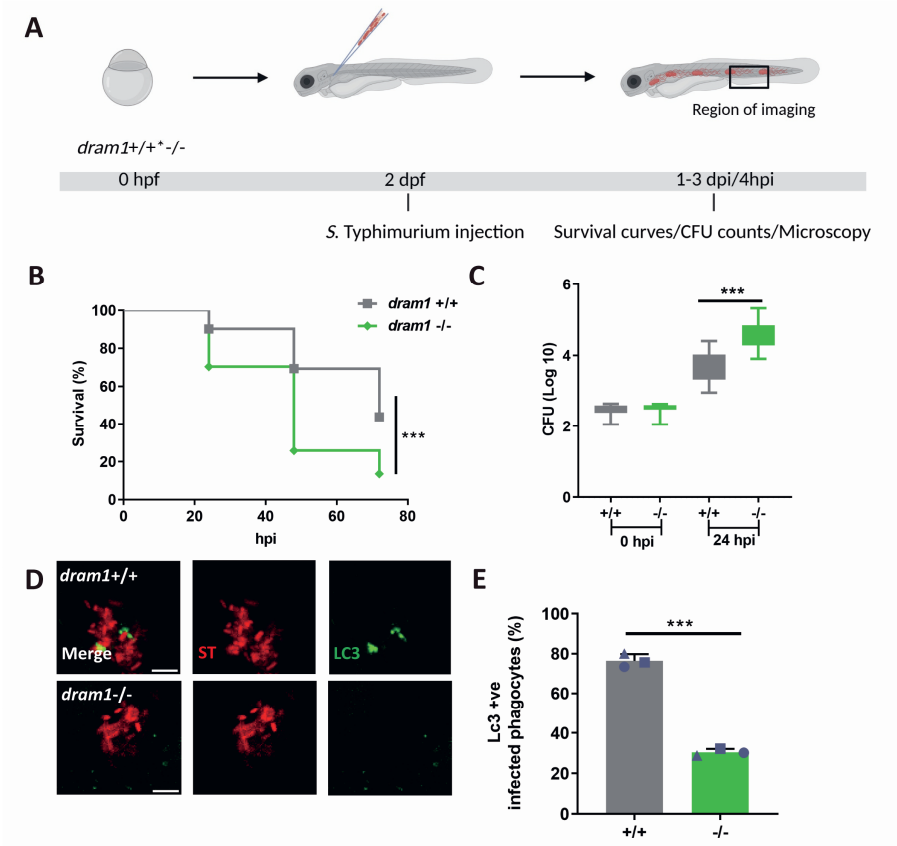


**Figure 3: GFP-Lc3 recruitment to *Salmonella* is impaired in *dram1* mutants in zebrafish.** (**A**) Workflow and timeline of experiments in B-E. (**B**) Survival curves of *dram1*+/+ and *dram1*-/- embryos infected with *S.* Typhimurium (n=150 embryos/group from three independent experiment). (**C**) CFU counts recovered from *dram1*+/+ and *dram1*- /- infected individuals (n=15 embryos/group from 3 three independent experiments). (**D**) Representative confocal micrographs of GFP-Lc3-*Salmonella* colocalization in *dram1*+/+ and *dram1*-/- embryos in *Tg(CMV:GFP-maplc3b1)* background. Scale bar = 5 µm (**E**) Quantification of GFP-Lc3-*Salmonella* colocalization in *dram1*+/+ and *dram1* -/- embryos (n= 15 embryos/group). The bar graph shows the data from three independent experiments, where the mean of each replicate is indicated with a different symbol. Error bars represent SD. Statistical significance of survival curves data is assessed by Cox proportional hazards model with log rank test. Statistical significance of CFU counts and GFP-Lc3-*Salmonella* colocalization data is analyzed by unpaired t-test. (***p<0.001).

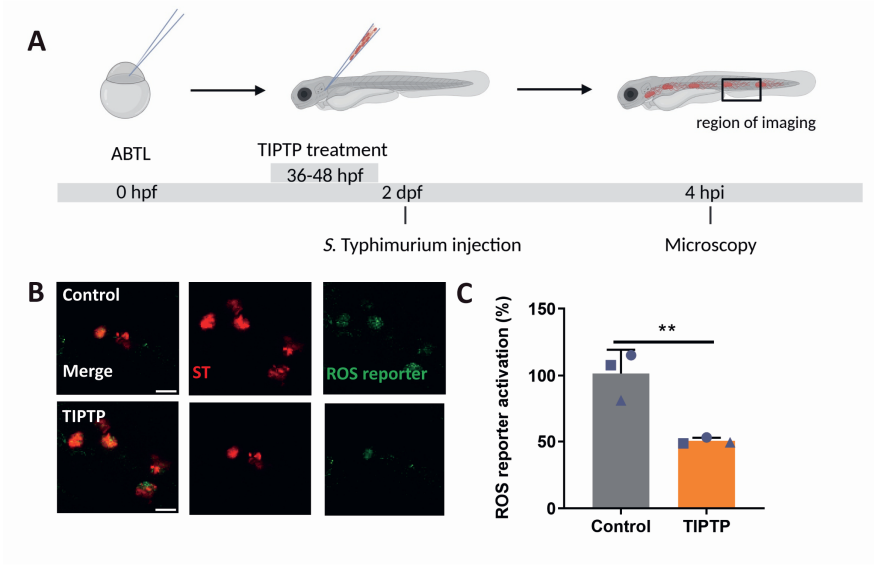


**Figure 4: ROS generation is inhibited by TIPTP in zebrafish.** (**A**) Workflow and timeline of experiments in B-C. (**B**) Representative micrographs for control and TIPTP-treated embryos infected with a *Salmonella* biosensor strain for ROS. Images were taken at 4 hpi. Scale bar = 10 µm (**C**) Quantification of the ROS reporter activation (GFP intensity compared to constitutive mCherry intensity). The bar graph shows the data from three independent experiments, where the mean of each replicate is indicated with a different shape. (n=15 embryos per group). Statistical significance is analyzed by unpaired t-test. (**p<0.01). Error bars represent the SD.

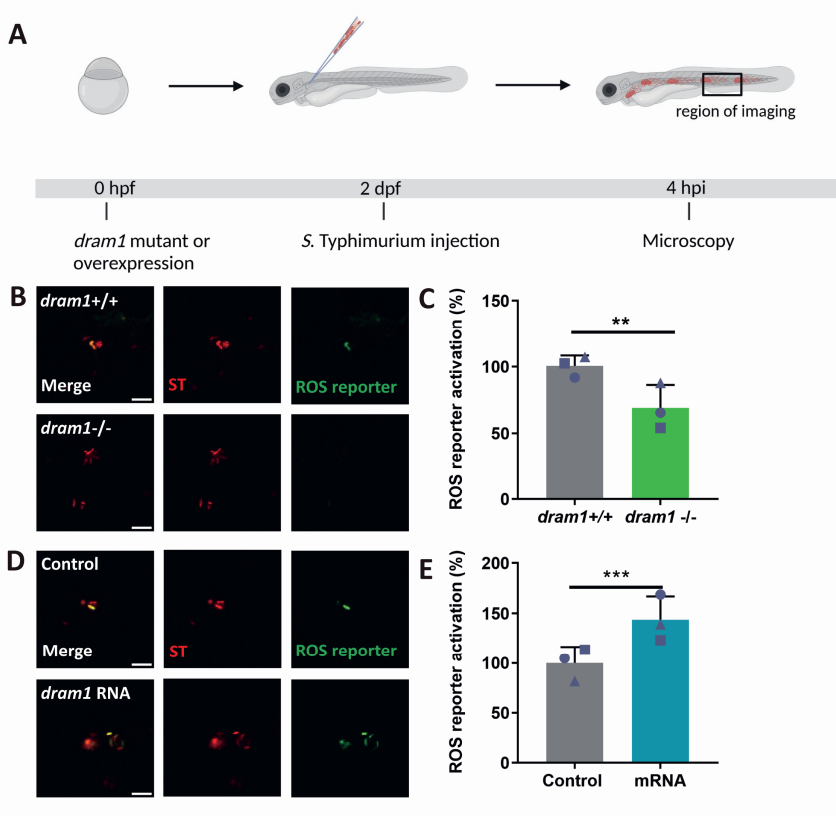


**Figure 5: ROS generation is mediated by Dram1 during *Salmonella* infection in the zebrafish model.** (**A**) Workflow and timeline of experiments in B-E. (**B**). Representative micrographs for *dram1*+/+ and *dram1*-/- embryos infected with a *Salmonella* biosensor strain for ROS. Images were taken at 4 hpi. Scale bar = 5 µm (**C**) Quantification of the ROS reporter activation (GFP intensity compared to constitutive mCherry intensity) in *dram1+/+* and *dram1-/-* embryos. (**D**) Representative micrographs for control and *dram1* mRNA overexpression embryos, infected with a *Salmonella* biosensor strain for ROS. Scale bar = 10 µm (**E**) Quantification of the ROS reporter activation (GFP intensity compared to constitutive mCherry intensity) in control and *dram1* mRNA overexpression embryos. Bar graphs show the data from three independent experiments, where the mean of each replicate is indicated with a different shape (n=15 embryos per group). Error bars represent the SD. Statistical significance is analyzed by is analyzed by unpaired t-test. (**p<0.01; ***p<0.001).

**DRAM1 enhances the LAP response of murine macrophages to *S.* Typhimurium**

To determine if the LAP response to *S.* Typhimurium is shared between zebrafish and a mammalian model, we utilized the mouse RAW 264.7 macrophage cell line. First, we incubated RAW 264.7 macrophages with the LAP inhibitor, TIPTP, and subsequently infected the cells with *S.* Typhimurium expressing the ROS biosensor **(Figure 6A)**. Activation of the ROS biosensor was reduced in presence of TIPTP **(Figure 6B,C)**. In agreement, TIPTP also reduced LC3 immunostaining in *S.* Typhimurium-infected macrophages **(Figure 6D,E)**. Next, we tested the effect of DRAM1 loss-and-gain-of-function **(Figure 7A)**. Knockdown of *Dram1* via lentivirus transfection of shRNA (**Fig S3**) (Banducci-Karp et al., 2023) resulted in lower levels of ROS biosensor activation **(Figure 7B,C)**, while overexpression of *Dram1* (**Fig S4**) led to higher ROS biosensor activity **(Figure 7D, E)**. To confirm the effect of DRAM1 on ROS production by LAP, we then utilized isoluminol, a cell-impermeable chemiluminescent chemical, which makes it possible to detect exclusively the ROS that is produced in the lumen of vesicles derived from endocytosis and phagocytosis (Herb and Schramm, 2021). We found that similar to the results obtained with the ROS biosensor strain, knockdown of *Dram1* produced less ROS, and overexpression of *Dram1* increased ROS production after infection **(Figure 7F)**. As a control, the different cell lines produced similar levels of ROS after stimulation by PMA **(Figure 7G)** or under non-infected conditions **(Fig S5)**. In agreement, LC3 colocalization with *Salmonella* **(Figure 8A)** was reduced in the *Dram1* knockdown cells **(Figure 8B,C)** and increased with overexpression of *Dram1* **(Figure 8D,E)**. In conclusion, RAW 246.7 macrophages target *S.* Typhimurium similarly by LAP as macrophages in the zebrafish host, and this response is stimulated by DRAM1/Dram1 in both systems.

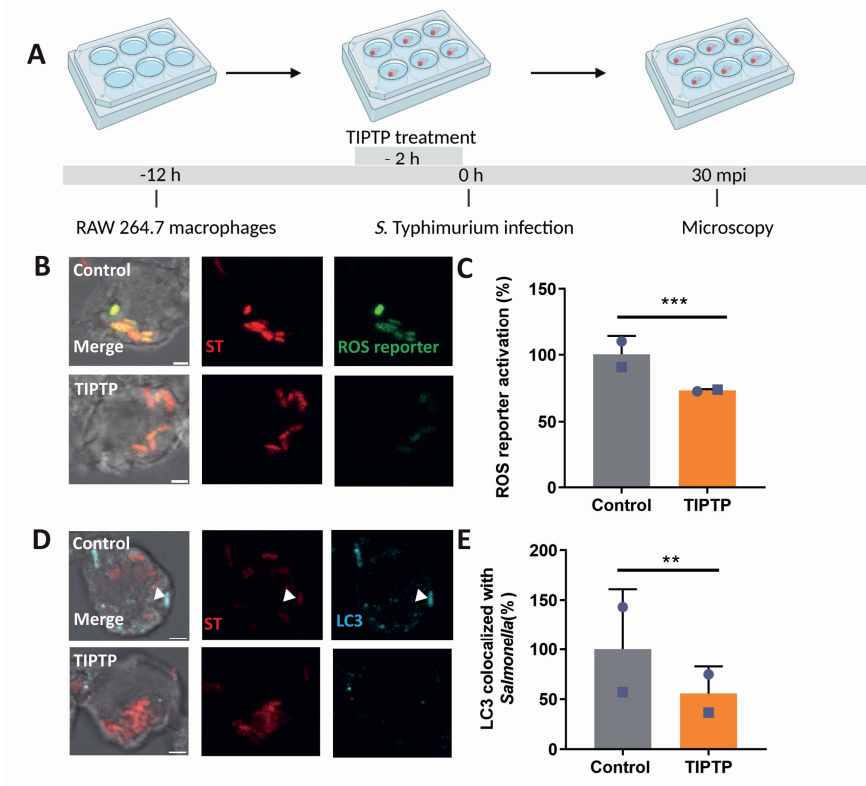


**Figure 6: ROS generation and LC3 colocalization with *Salmonella* are inhibited by TIPTP in RAW 264.7 macrophages.** (**A**) Workflow and timeline of experiments (**B**). Representative micrographs for control and TIPTP-treated cells infected with a *Salmonella* biosensor strain for ROS. Scale bar = 2 µm. (**C**) Quantification of the ROS reporter activation (GFP intensity compared to constitutive mCherry intensity). (**D**) Representative confocal micrographs of LC3 immunostaining colocalized with *mCherry*-expressing *S*. Typhimurium. Scale bar = 2 µm. (**E**) Quantification of LC3-*Salmonella* colocalization. Bar graphs show the data from two independent LC3 immunostaining experiments, where the mean of each replicate is indicated with a different symbol (n=24 regions of interest per group). Statistical significance is analyzed by one-way ANOVA and pairwise comparison with Dunnett correction.
( **p<0.01; ***p<0.001). Error bars represent the SD.

**Figure 7: DRAM1 promotes ROS generation during *Salmonella* infection in RAW 264.7 macrophages.** (**F**) Isoluminol measurement of ROS production in *Dram1* knockdown, overexpression, and control cells after infection or stimulation with PMA (**G**). Graphs show the data from one replicate out of two independent experiments. Statistical significance is analyzed by one-way ANOVA and pairwise comparison with Dunnett correction. *p<0.05, **p<0.01; ***p<0.001). Error bars represent the SD.

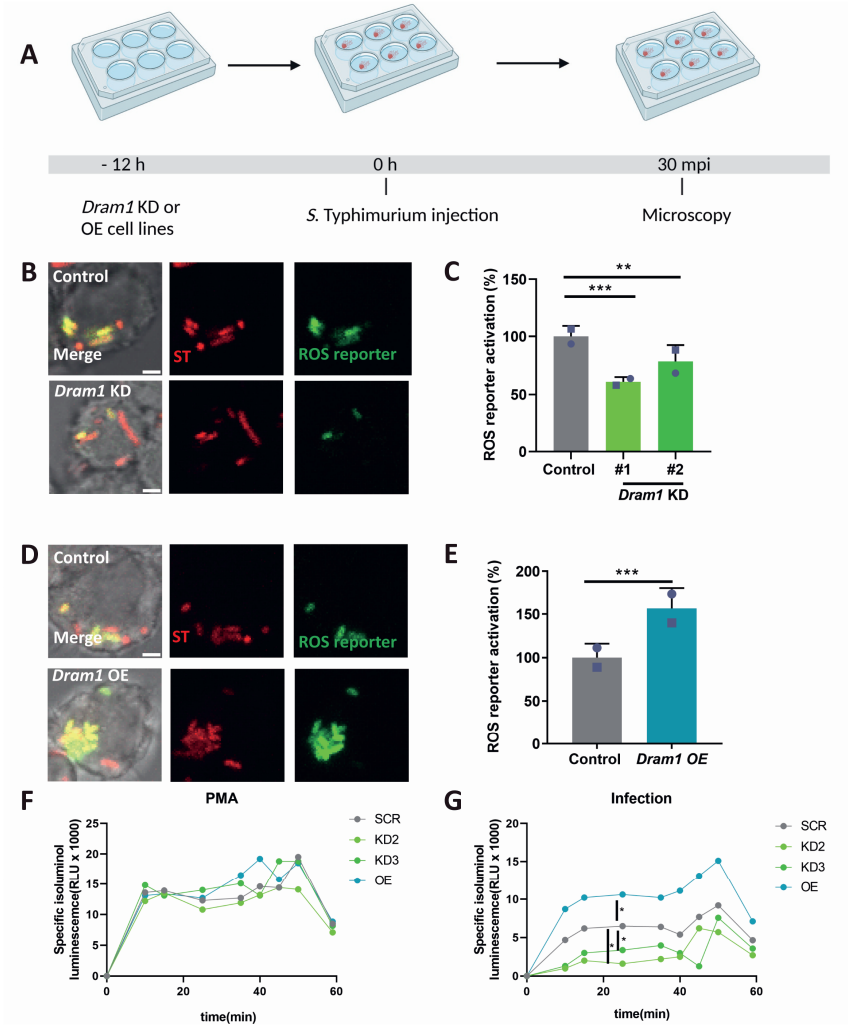


**Figure 7: DRAM1 promotes ROS generation during *Salmonella* infection in RAW 264.7 macrophages.** (**A**) Workflow and timeline of experiments (**B**) Representative micrographs for *Dram1* control and knockdown (KD) cells, infected with a *Salmonella* biosensor strain for ROS. Scale bar = 2 µm. (**C**) Quantification of the ROS reporter activation (GFP intensity compared to constitutive mCherry intensity) in *Dram1* control and knockdown (KD) cells. (**D**) Representative micrographs for *Dram1* control and overexpression (OE) cells infected with a *Salmonella* biosensor strain for ROS. Scale bar = 2 µm. (**E**) Quantification of the ROS reporter activation (GFP intensity compared to constitutive mCherry intensity) in *Dram1* control and overexpression (OE) cells. Bar graphs show the data from two independent experiments, where the mean of each replicate is indicated with a different symbol (n=24 regions of interest per group).

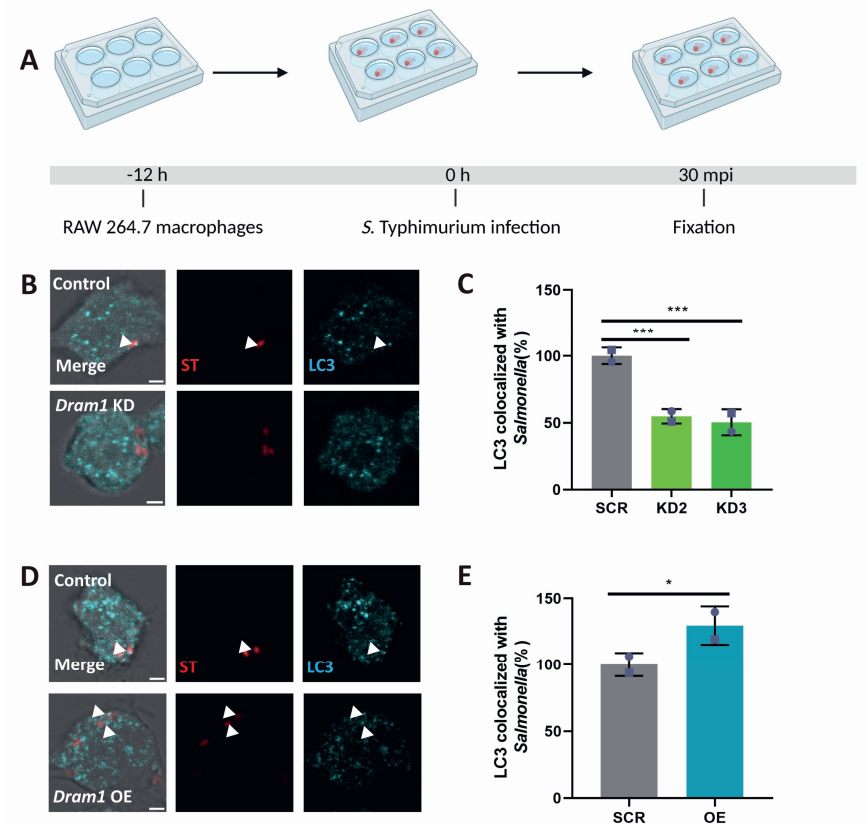


**Figure 8: DRAM1 increases LC3 colocalization with *Salmonella* in RAW 264.7 macrophages.** (**A**) Workflow and timeline of experiments (**B**). Representative micrographs of LC3 immunostaining colocalized with *mCherry*-expressing *S*. Typhimurium in *Dram1* knockdown cells infected with a *Salmonella*. Scale bar = 2 µm. (**C**) Quantification of LC3-*Salmonella* colocalization. (**D**) Representative confocal micrographs of LC3 immunostaining colocalized with *mCherry*-expressing *S*. Typhimurium in control and in *Dram1* overexpression cells. Scale bar = 2 µm. (**E**) Quantification of LC3-*Salmonella* colocalization. Bar graphs show the data from two independent LC3 immunostaining experiments, where the mean of each replicate is indicated with a different symbol (n=24 regions of interest per group). Statistical significance is analyzed by one-way ANOVA and pairwise comparison with Dunnett correction. ( *p<0.05; **p<0.01; ***p<0.001). Error bars represent the SD.

## Discussion

In this study, we have used zebrafish and murine RAW 264.7 macrophage infection models to demonstrate that the autophagy modulator Dram1/DRAM1 promotes host resistance to *Salmonella* infection. This work extends our previous finding that Dram1 mediates autophagic host defense during mycobacterial infection in the zebrafish tuberculosis model and in murine macrophages. Importantly, our study implicates Dram1/DRAM1 in an infection context where LAP is the predominant autophagic host defense response.

*S. Typhimurium* is vulnerable to both xenophagy and LAP, and employs its virulence factor SopF to suppress both these host pathways (Hooper et al., 2022; Xu et al., 2019). In the zebrafish infection model, macrophages target *S.* Typhimurium almost exclusively by LAP (Masud et al., 2019a). Depletion of essential LAP factors, including Rubicon and the NADPH oxidase component Cyba, abolishes GFP-Lc3 colocalization with *S.* Typhimurium and prevents activation of a bacterial ROS biosensor gene (Masud et al., 2019a). In the present study, we used a chemical approach to strengthen the previous genetic evidence for LAP and utilized TIPTP to interrupt the NADPH oxidase-Rubicon axis (Kim et al., 2020). Consistent with the involvement of LAP, we detected less activation of the bacterial ROS biosensor in both zebrafish and RAW 264.7 macrophages upon treatment with TIPTP. The ability of RAW 264.7 macrophages to respond to bacterial infections by LAP is in line with previous infection studies with *Escherichia coli* and *Burkholderia pseudomallei* (Gong et al., 2011; Sanjuan et al., 2007). Furthermore, the LAP response to *S.* Typhimurium has been confirmed in human cells (Hooper et al., 2022). DRAM1 has been shown to promote autophagy and autophagic flux, but has not previously been implicated in LAP (Crighton et al., 2006; Zhang et al., 2013). Here, we show that the LAP-associated ROS response is inhibited by knockdown or mutation of *dram1/Dram1* in zebrafish and murine macrophages, suggesting that Dram1/DRAM1 is required for the targeting of *S.* Typhimurium by LAP. This Dram1/DRAM1-mediated process is host-protective, since we found that *dram1*-deficient zebrafish embryos are more susceptible to *S.* Typhimurium infection and that *dram1* overexpression promotes host resistance.

The molecular mechanism by which Dram1/DRAM1 promotes autophagic processes is currently unknown. Our data show that Dram1/DRAM1 is required not only for Lc3/LC3 recruitment but also for the ROS response in phagosomes. This suggests that Dram1/DRAM1 functions upstream of

Rubicon, which has been shown to stabilize the NADPH oxidase. An attractive hypothesis is that Dram1/DRAM1 interacts directly with components of the Beclin1-VPS34-UVRAG-Rubicon complex to promote the association of Rubicon with phagosomes. This hypothesis is consistent with a recent study on a member of the human DRAM family, DRAM2, which has been shown to stimulate autophagy by disrupting the association of Rubicon with the Beclin1/UVRAG complex (Kim et al., 2011). The displacement of Rubicon relieves its inhibitory function from this complex and thereby promotes the activity of the class III phosphatidylinositol 3-kinase, VPS34, which is required for autophagosome formation and maturation. If Dram1/DRAM1 functions by a similar mechanism in the response to *Salmonella* infection, disruption of the Rubicon-Beclin1/Uvrag interaction would liberate Rubicon to associate with the *Salmonella*-containing phagosomes. This hypothesis would explain how Dram1/DRAM1 is able to stimulate autophagy and LAP at the same time. Another attractive hypothesis is that Dram1/DRAM1 stimulates the maturation of autophagosomes and LAPosomes by associating with lysosomal proteins, such as LAMP1 and LAMP2, similar to DRAM2 (Kim et al., 2011). Lysosomal markers, including LAMP1, Rab7a and V-ATPase, have been found to associate with phagosomes prior to LC3 recruitment and acidification (Hooper et al., 2022). Furthermore, the V-ATPase has been identified as a universal driver of LAP and other forms of CASM by recruiting ATG16L, a function that is separate from its subsequent role in driving acidification (Hooper et al., 2022). Therefore, the current view on LAP/CASM activation supports a model whereby DRAM1 may associate with lysosomal factors both before and after LC3 recruitment, allowing it to promote LAP initiation as well as LAPosome maturation. This is consistent with previous studies implicating DRAM1 in vesicle fusion and maturation during canonical autophagy (Banducci-Karp et al., 2023; Geng et al., 2020; van der Vaart et al., 2020; Zhang et al., 2013).

In addition to promoting LAP, it is likely that the activity of Dram1/DRAM1 can enhance other autophagic mechanisms against intracellular *Salmonella*, including the selective autophagy process that is mediated by ubiquitin receptors. Selective autophagy has been shown to function as an important defense mechanism against *Salmonella* in epithelial cells, which this pathogen enters by active invasion (Huang et al., 2009). Selective autophagy specifically targets cytosolic bacteria or detects membrane damage on the bacterial replication niche. In both zebrafish and RAW 264.7 macrophages, we have shown that this response is elicited by the escape of *M. marinum* from phagosomes (Banducci-Karp et al., 2023; van der Vaart et al., 2014). The above proposed interaction of Dram1/DRAM1 with Rubicon is consistent with

positive effects on selective autophagy as well as LAP. In addition, the microbicidal capacity of Lc3/LC3-marked bacterial compartments might be enhanced by Dram1/DRAM1 activity, regardless of whether these compartments are of autophagosomal or phagosomal origin. This could be facilitated by delivery of ubiquitinated antimicrobial peptides through fusion with autophagosomes, which are present in increased numbers when Dram1 is overexpressed (Ponpuak et al., 2010; van der Vaart et al., 2014).

Different members of the DRAM family might have partially overlapping functions in host defense. In addition to a single copy of *dram1*, the zebrafish has two copies of the gene for Dram2, *dram2a* and *dram2b*. Based on our RNA sequencing data of leukocyte populations sorted from zebrafish larvae, *dram1* is the most abundantly expressed gene in macrophages, while the expression level of *dram2b* is at least 10-fold lower and *dram2a* is not detectably expressed (Rougeot et al., 2019). Furthermore, we have only found expression of *dram1* to be inducible by infection (Benard et al., 2014; Stockhammer et al., 2010). Our study did not provide any indication that other members of the zebrafish Dram family might be involved in LAP, since mutation of *dram1* abolished ROS biosensor activation in the *Salmonella*-containing phagosomes almost completely. However, the possible role of Dram2a/b in zebrafish host defense requires further investigation in the light of the recent report that *Mycobacterium tuberculosis* evades autophagy by inducing the expression of microRNAs (miR144* and miR-125b-5p) that target human *DRAM2* (Kim et al., 2017). This study has revealed that DRAM2 enhances antimicrobial activity in human monocyte derived macrophages, similar to the functions that we have shown for mouse DRAM1 in *M. marinum*-infected mouse macrophages and for zebrafish Dram1 during *in vivo* infections with *M. marinum* and *S*. Typhimurium (Banducci-Karp et al., 2023; Zhang et al., 2020). Therefore, accumulating evidence positions the members of the DRAM family as key players in autophagic defense against intracellular pathogens and it will be of great interest to further explore how these autophagy/LAP modulators might work in concert and how they could be therapeutically targeted.

## Materials and methods

### Zebrafish lines and maintenance

Zebrafish were handled in compliance with local animal welfare regulations and international guidelines specified by the EU Animal Protective Directive 2010/63/EU and maintained according to standard protocols (zfin.org). All studies were performed on embryos/larvae before the free feeding stage. Fish lines used for this study are AB/TL (a cross between wild type strains AB and Tuebingen Longfin; zfin.org), transgenic lines *Tg(CMV:GFP-map1lc3b)* and *dram1-/-* and *dram1*+/+ in *Tg(CMV:GFP-map1lc3b)* backgrounds (Zhang et al., 2020). Embryos from adult fish were handled and treated pre-infection and post infection as described (Masud et al., 2019a).

### RAW 264.7 macrophages culture

The mouse macrophage-like cell line RAW 264.7 was maintained in high glucose Dulbecco's modified Eagle's medium (DMEM, Gibco, D6546) supplemented with 10% fetal calf serum (Gibco, F2442) and 1% GlutaMAX (Gibco, 35050061), at 37 °C under a humidified atmosphere of 95% air and 5% CO2.

### Bacterial strains and infection experiments

*S.* Typhimurium SL1344 strains were used for this study, constitutively expressing *mCherry* or the *mCherry* marker in combination with a GFP biosensor for ROS (p*katGp-gfpOVA)* (Burton et al., 2014). Culturing of bacteria, preparation of infection inocula and infection delivery were performed as described before (Masud et al., 2019a). Briefly, bacteria were resuspended in PBS supplemented with 2% polyvinylpyrrolidone-40 to obtain the low dose (200-400 CFU, for survival curves and CFU counts experiments) or high dose (2000-4000 CFU, for imaging experiments). Bacterial inoculum was injected systemically into the caudal vein of 2 dpf anaesthetized embryos. Survival of infected embryos was recorded at 24 hour intervals. For infection of RAW 264.7 macrophages, cells were infected with a multiplicity of infection of 10, and immediately centrifuged at 500 g for 10 min, as described in (Stamm et al., 2003), and subsequently incubated at 37˚C for 30 min.

**TIPTP experiments**

The TIPTP inhibitor was synthesized and kindly provided by Dr. Sun-Joon Min and Dr. Chul-Su Yang (Kim et al., 2020). For use in zebrafish experiments, embryos were treated with 0.1 µM TIPTP diluted in egg water from 36 hpf to 48 hpf, then transferred to fresh egg water for *S.* Typhimurium injection. 4h after injection, fish were taken to confocal for imaging. For experiments with RAW 264.7 macrophages, cells were treated with 10 µM TIPTP for 2 hours before infection. After 30 minute infection, cells were washed twice with PBS to remove extracellular bacteria and fixed with Pierce™ 4% formaldehyde for 15 minutes for imaging. To check the effect on *S.* Typhimurium growth *in vitro*, the bacteria were cultured overnight and diluted with LB medium to OD600 of 0.2, treated with 0, 0.01, 0.1, 1, 10, and 100 µM of TIPTP, and OD600 was measured at different time points.

**Determination of bacterial (CFU) counts in zebrafish**

The CFU counts from infected zebrafish embryos were determined as described in (Masud et al., 2019a). Briefly, homogenized infected embryos were serially diluted and plated out on solid media containing 90 µg/ml streptomycin, 50 µg/ml kanamycin and 100 µg/ml ampicillin to enumerate bacterial colonies.

**Dram1 knockdown and overexpression experiments in zebrafish**

Dram1 expression was altered by injecting 1 nl of a 0.1 mM solution of a previously described antisense morpholino MO1-dram1 (AAGGCTGGAAAACAAACGTACAGTA) or by injecting at a concentration of 100 pico grams of *dram1* mRNA in 1 nl (van der Vaart et al., 2014).

**DRAM1 knockdown and overexpression in macrophages**

The shRNA knockdown of *Dram1* in RAW 264.7 macrophages has been previously described (Banducci-Karp et al., 2023). In this study we used two independent knockdown lines, corresponding to lines KD2 and KD3 in our previous study (Banducci-Karp et al., 2023). To generate *Dram1* construct for overexpression, primers were designed with adaptors F: GCGGATCCGCCACCATGCTGTGCTTCCTCAGGGGAATGGCTTTCG; R: GCTCTAGATCAAAAGTCGTCATTGATTTCTGTGG for PCR using *Dram1* ORF clone template (OriGene, MR220640). Amplified fragment was verified by gel

electrophoresis and purified with GenElute Gel Extraction Kit (Sigma-Aldrich, SLBT 5695). Vector (pLenti CMV TO eGFP Puro, w159-1) was cut at the BamHI and Xbal restriction site and ligated with the *Dram1* fragment by using T4 DNA ligase (NEB, M0202) . The ligated *Dram1* plasmid was transformed to DH5α competent cells. Colonies were picked and transformation was verified by PCR and sanger sequencing. To generate lentiviral particles with a *Dram1* overexpression construct, low passage HEK293T cells were seeded in a 25 cm2 culture flask one day prior to transfection. For assembly of lentiviral particles, virulent plasmid pMD2.G (Addgene, 12259), packing plasmid psPAX (Addgene, 12260) and transfer plasmid containing *Dram1* were used at final concentrations of 0,72 pmol, 1,3 pmol and 1,64 pmol, respectively. The plasmids were mixed in 250 µL of DMEM without fetal calf serum (FCS; Gibco). Liposomal transfectant lipoD293 (Signagen, SL100668) was diluted in another 250 µL of DMEM without FCS. The plasmid mixture and diluted transfectant were then combined, mixed and incubated for 20 min. The liposomal complex was added dropwise to the medium of the HEK293T cells. Cells were incubated for 16 h to allow for efficient transfection. Next, the medium was replaced with 7 ml DMEM containing 25 µM HEPES and the culture was incubated for 2 days. Viral particles were then harvested through collection of the culture supernatant. Lentiviral supernatant was aliquoted and kept at -80°C prior to use. The day before transduction, $1x10^6$ low passage RAW 264.7 cells were seeded in 6 well plates in DMEM-high glucose with 10% FCS and incubated overnight at 37°C with 5% $CO_2$. 24 h later, cells were transduced with *Dram1*-containing lentivirus supplemented with 8 µg/ml polybrene (Sigma-Aldrich, TR1003), and incubated at 37°C with 5% $CO_2$. Medium was refreshed 24 h after transduction. After 48 h of transduction, 3 µg/ml puromycin (Gibco, A1113803) was added. Every 2-3 days, the medium was replaced until cells were 80-90% confluent. After around 7-10 days, all the non-transduction cells have died, and the puromycin-resistant were used for experiments. *Dram1* overexpression in these cells was verified by qPCR analysis.

**Quantitative PCR**

qPCR was done according to the methods described by Banducci-Karp et al (Banducci-Karp et al., 2023). Briefly, total RNA was extracted by TRIzol (Invitrogen, 15596018). 0.5 µg of total RNA was then transcribed as cDNA with iScript cDNA synthesis kit (Bio-Rad, 1708890). The mRNA expression level was determined by quantitative real-time PCR using iQSYBR Green

Supermix (Bio-Rad, 1725271). For RAW 264.7 macrophages, *Dram1* primers used are as follows: forward: 5'-CCAGCTTCTTGGTCCGACG-3', reverse: '5-GGGAGAAAGGGGTTGACGTG-3'. *Gapdh* was used as the housekeeping gene : forward: 5'- ATGGTGAAGGTCGGTGTGAA-3', reverse: '5-CTGGAACATGTAGACCATGT -3'. For zebrafish, *dram1* primers used are as follows: forward: 5'-GTGCCCCCTACTCTGAACAA-3'; reverse: 5'-GCGGTATCCGATCACACTCT-3'. *tbp* was used as the housekeeping gene: forward: 5'-CCTGCCCATTTTCAGTC-3', reverse: 5'-TGTTGTTGCCTCTGTTGCTC-3'.

**Western blotting**

Cells were harvested, lysed by ultrasonication, and incubated with Laemmli SDS sample buffer (Thermo Fisher, J60015) at 37 °C for 10 min. Western blotting was performed using 10% polyacrylamide gels, followed by protein transfer to nitrocellulose membrane (Amersham Protran, GE10600001, Sigma-Aldrich). After the transfer, the membrane was placed in stripping buffer (2% SDS, 100 mM b-mercaptoethanol, and 62.5 mM Tris–HCl) at 55 °C for 15 min to expose the epitope. Membranes were then blocked with 3% BSA in 1× Tris-buffered saline (TBS) solution, with 0.1% Tween-20 (TBST), before incubating with primary and secondary antibodies: polyclonal anti-rabbit DRAM1 (1:1000) (Aviva systems biology, ARP47432- P050), β-actin (1:1000)( Cell Signaling, 4967S), as well as anti-rabbit IgG, and HRP-linked antibody (1:1000) (Cell Signaling, 7074S). Digital images were acquired using the Bio-Rad Universal Hood II imaging system (720BR/01565 UAS). Band intensities were quantified with densitometric analysis using Image Lab software and were normalized to β-actin as a loading control.

**Immunofluorescence of RAW 264.7 macrophages**

Cells were fixed in 4% PFA for 15 min and after fixation, cells were permeabilized with 0.2% Saponin (Sigma-Aldrich, 47036) in PBS for 15 min, and then blocked with 3% bovine serum albumin (BSA) (Sigma-Aldrich, A4503) in PBS for 1 h at room temperature. Next, cells were incubated with the primary antibody LC3 (1:500) (Novus Biologicals, NB100-2331) for 1 hour at room temperature. Secondary antibody goat-anti-rabbit Alexa Fluor Plus 647 (1:1000) (Invitrogen, A-21245) was then added for detection of the primary antibodies. Prolong Gold Antifade Reagent (Invitrogen, P36966) was used for mounting onto glass slides. Between each step, cells were washed four times with PBS for 5 min each.

**Quantification of ROS production by isoluminol**

Cells were seeded the day before isoluminol measurement. Prior to the infection, the baseline signal was measured. The cells were then infected with *Salmonella* or stimulated with 1 ng/mL PMA (InvivoGen, 16561-29-8), and incubated with 50 mM isoluminol (TGI, A5300) and 3.2 U/mL horseradish peroxidase (Thermo Scientific, 31490) at 37 °C. Isoluminol luminescence was measured by Tecan Infinite M 1000 microplate reader.

**Image acquisition and image analysis**

Infected zebrafish embryos or RAW 264.7 macrophages were fixed for image acquisitions to quantify GFP-Lc3-*Salmonella* colocalization and ROS biosensor activation. A 63x/40x water immersion objective (NA 1.3 or NA 0.8) with a Leica TCS SPE and SP8 confocal microscope system was used. When imaging zebrafish embryos, the selected region of interest was an area in the caudal hematopoietic tissue region in the ventral part of the tail, close to the site of injection. During imaging of RAW 264.7 macrophages cultured on glass slides, regions of interest were randomly selected by navigating over the slides in a zig-zag pattern. GFP-Lc3-*Salmonella* colocalization were quantified by visual stack-by-stack inspection of the confocal Z-stack images. For ROS biosensor quantification, the intensity of the mCherry signal from *S.* Typhimurium was quantified as the area of infection using Image J. The mCherry signal was then used as a 'mask' to quantify the fluorescence intensity of the GFP signal, which represents ROS production. ROS activation was then determined by calculating the ratio between the intensity of the GFP signal and the intensity of the mCherry signal, in agreement with previous work (Xie et al., 2021). Max projections in the overlay channels were used for representative images.

**Statistical analysis**

All data sets were analyzed with Prism 8 software. Survival curves were analyzed with Log rank (Mantel-Cox) test. For CFU counts, data analysis was performed on Log-transformed data. Data of GFP-Lc3-positive infected phagocytes and ROS biosensor-positive phagocytes were analyzed with unpaired parametric t-test between two groups and for multiple groups the one-way ANOVA test was performed and corrected with Dunnett comparisons as indicated in figure legend.

## References


Banducci-Karp, A., Xie, J., Engels, S.A.G., Sarantaris, C., van Hage, P., Varela, M., Meijer, A.H., and van der Vaart, M. (2023). DRAM1 Promotes Lysosomal Delivery of Mycobacterium marinum in Macrophages. cells *12*, 828.

Beaumatin, F., O'prey, J., Barthet, V.J., Zunino, B., Parvy, J.-P., Bachmann, A.M., O'prey, M., Kania, E., Gonzalez, P.S., and Macintosh, R. (2019). mTORC1 activation requires DRAM-1 by facilitating lysosomal amino acid efflux. Molecular cell *76*, 163-176. e168.

Benard, E.L., Roobol, S.J., Spaink, H.P., and Meijer, A.H. (2014). Phagocytosis of mycobacteria by zebrafish macrophages is dependent on the scavenger receptor Marco, a key control factor of pro-inflammatory signalling. Developmental & Comparative Immunology *47*, 223-233.

Boyle, K.B., and Randow, F. (2013). The role of 'eat-me'signals and autophagy cargo receptors in innate immunity. Current opinion in microbiology *16*, 339-348.

Burton, N.A., Schürmann, N., Casse, O., Steeb, A.K., Claudi, B., Zankl, J., Schmidt, A., and Bumann, D. (2014). Disparate impact of oxidative host defenses determines the fate of Salmonella during systemic infection in mice. Cell host & microbe *15*, 72-83.

Chen, C., Liang, Q.Y., Chen, H.K., Wu, P.F., Feng, Z.Y., Ma, X.M., Wu, H.R., and Zhou, G.Q. (2018). DRAM1 regulates the migration and invasion of hepatoblastoma cells via autophagy-EMT pathway. Oncology Letters *16*, 2427-2433.

Crighton, D., Wilkinson, S., O'Prey, J., Syed, N., Smith, P., Harrison, P.R., Gasco, M., Garrone, O., Crook, T., and Ryan, K.M. (2006). DRAM, a p53-induced modulator of autophagy, is critical for apoptosis. Cell *126*, 121-134.

Deretic, V., Saitoh, T., and Akira, S. (2013). Autophagy in infection, inflammation and immunity. Nature Reviews Immunology *13*, 722-737.

Deretic, V., Singh, S., Master, S., Harris, J., Roberts, E., Kyei, G., Davis, A., De Haro, S., Naylor, J., and Lee, H.H. (2006). Mycobacterium tuberculosis inhibition of phagolysosome biogenesis and autophagy as a host defence mechanism. Cellular microbiology *8*, 719-727.

Durgan, J., and Florey, O. (2021). A new flavor of cellular Atg8-family protein lipidation–alternative conjugation to phosphatidylserine during CASM. Autophagy *17*, 2642-2644.

Durgan, J., Lystad, A.H., Sloan, K., Carlsson, S.R., Wilson, M.I., Marcassa, E., Ulferts, R., Webster, J., Lopez-Clavijo, A.F., and Wakelam, M.J. (2021). Non-canonical autophagy drives alternative ATG8 conjugation to phosphatidylserine. Molecular cell *81*, 2031-2040. e2038.

Galavotti, S., Bartesaghi, S., Faccenda, D., Shaked-Rabi, M., Sanzone, S., McEvoy, A., Dinsdale, D., Condorelli, F., Brandner, S., and Campanella, M. (2013). The autophagy-associated factors DRAM1 and p62 regulate cell migration and invasion in glioblastoma stem cells. Oncogene *32*, 699-712.

Geng, J., Zhang, R., Yuan, X., Xu, H., Zhu, Z., Wang, X., Wang, Y., Xu, G., Guo, W., and Wu, J. (2020). DRAM1 plays a tumor suppressor role in NSCLC cells by promoting lysosomal degradation of EGFR. Cell death & disease *11*, 1-15.
Gong, L., Cullinane, M., Treerat, P., Ramm, G., Prescott, M., Adler, B., Boyce, J.D., and Devenish, R.J. (2011). The Burkholderia pseudomallei type III secretion system and BopA are required for evasion of LC3-associated phagocytosis. PloS one *6*, e17852.
Grijmans, B.J., van der Kooij, S.B., Varela, M., and Meijer, A.H. (2022). LC3-associated phagocytosis and the arms race against bacterial pathogens. Frontiers in Cellular and Infection Microbiology, 1343.
Guan, J., Zhang, X., Sun, W., Qi, L., Wu, J., and Qin, Z. (2015). DRAM1 regulates apoptosis through increasing protein levels and lysosomal localization of BAX. Cell death & disease *6*, e1624-e1624.
Herb, M., and Schramm, M. (2021). Functions of ROS in macrophages and antimicrobial immunity. Antioxidants *10*, 313.
Hooper, K.M., Jacquin, E., Li, T., Goodwin, J.M., Brumell, J.H., Durgan, J., and Florey, O. (2022). V-ATPase is a universal regulator of LC3-associated phagocytosis and non-canonical autophagy. Journal of Cell Biology *221*.
Huang, J., and Brumell, J.H. (2014). Bacteria–autophagy interplay: a battle for survival. Nature Reviews Microbiology *12*, 101-114.
Huang, J., Canadien, V., Lam, G.Y., Steinberg, B.E., Dinauer, M.C., Magalhaes, M.A., Glogauer, M., Grinstein, S., and Brumell, J.H. (2009). Activation of antibacterial autophagy by NADPH oxidases. Proceedings of the national academy of sciences *106*, 6226-6231.
Hubber, A., Kubori, T., Coban, C., Matsuzawa, T., Ogawa, M., Kawabata, T., Yoshimori, T., and Nagai, H. (2017). Bacterial secretion system skews the fate of Legionella-containing vacuoles towards LC3-associated phagocytosis. Scientific reports *7*, 1-17.
Kim, J., Kundu, M., Viollet, B., and Guan, K.-L. (2011). AMPK and mTOR regulate autophagy through direct phosphorylation of Ulk1. Nature cell biology *13*, 132-141.
Kim, J.K., Lee, H.-M., Park, K.-S., Shin, D.-M., Kim, T.S., Kim, Y.S., Suh, H.-W., Kim, S.Y., Kim, I.S., and Kim, J.-M. (2017). MIR144* inhibits antimicrobial responses against Mycobacterium tuberculosis in human monocytes and macrophages by targeting the autophagy protein DRAM2. Autophagy *13*, 423-441.
Kim, Y.-R., Kim, J.-S., Gu, S.-J., Jo, S., Kim, S., Young Kim, S., Lee, D., Jang, K., Choo, H., and Kim, T.-H. (2020). Identification of highly potent and selective inhibitor, TIPTP, of the p22phox-Rubicon axis as a therapeutic agent for rheumatoid arthritis. Scientific reports *10*, 1-15.
Laforge, M., Limou, S., Harper, F., Casartelli, N., Rodrigues, V., Silvestre, R., Haloui, H., Zagury, J.-F., Senik, A., and Estaquier, J. (2013). DRAM triggers lysosomal membrane permeabilization and cell death in CD4+ T cells infected with HIV. PLoS pathogens *9*, e1003328.
Lei, Y., and Klionsky, D.J. (2022). The coordination of V-ATPase and ATG16L1 is part of a common mechanism of non-canonical autophagy (Taylor & Francis), pp. 2267-2269.

Levine, B., and Klionsky, D.J. (2004). Development by self-digestion: molecular mechanisms and biological functions of autophagy. Developmental cell *6*, 463-477.
Ligeon, L.-A., Pena-Francesch, M., Vanoaica, L.D., Núñez, N.G., Talwar, D., Dick, T.P., and Münz, C. (2021). Oxidation inhibits autophagy protein deconjugation from phagosomes to sustain MHC class II restricted antigen presentation. Nature communications *12*, 1-13.
Mah, L.Y., O'Prey, J., Baudot, A.D., Hoekstra, A., and Ryan, K.M. (2012). DRAM-1 encodes multiple isoforms that regulate autophagy. Autophagy *8*, 18-28.
Martinez, J. (2018). LAP it up, fuzz ball: a short history of LC3-associated phagocytosis. Current opinion in immunology *55*, 54-61.
Martinez, J., Malireddi, R., Lu, Q., Cunha, L.D., Pelletier, S., Gingras, S., Orchard, R., Guan, J.-L., Tan, H., and Peng, J. (2015). Molecular characterization of LC3-associated phagocytosis reveals distinct roles for Rubicon, NOX2 and autophagy proteins. Nature cell biology *17*, 893-906.
Masud, S., Prajsnar, T.K., Torraca, V., Lamers, G.E., Benning, M., Van Der Vaart, M., and Meijer, A.H. (2019a). Macrophages target Salmonella by Lc3-associated phagocytosis in a systemic infection model. Autophagy *15*, 796-812.
Masud, S., Van der Burg, L., Storm, L., Prajsnar, T.K., and Meijer, A.H. (2019b). Rubicon-dependent Lc3 recruitment to salmonella-containing phagosomes is a host defense mechanism triggered independently from major bacterial virulence factors. Frontiers in Cellular and Infection Microbiology *9*, 279.
Meijer, A.H., and van der Vaart, M. (2014). DRAM1 promotes the targeting of mycobacteria to selective autophagy. Autophagy *10*, 2389-2391.
Meng, C., Liu, Y., Shen, Y., Liu, S., Wang, Z., Ye, Q., Liu, H., Liu, X., and Jia, L. (2018). MicroRNA-26b suppresses autophagy in breast cancer cells by targeting DRAM1 mRNA, and is downregulated by irradiation Corrigendum in/10.3892/ol. 2021.12460. Oncology letters *15*, 1435-1440.
Mizushima, N. (2007). Autophagy: process and function. Genes & development *21*, 2861-2873.
Mizushima, N., Yamamoto, A., Matsui, M., Yoshimori, T., and Ohsumi, Y. (2004). In vivo analysis of autophagy in response to nutrient starvation using transgenic mice expressing a fluorescent autophagosome marker. Molecular biology of the cell *15*, 1101-1111.
Mostowy, S. (2013). Autophagy and bacterial clearance: a not so clear picture. Cellular microbiology *15*, 395-402.
Ponpuak, M., Davis, A.S., Roberts, E.A., Delgado, M.A., Dinkins, C., Zhao, Z., Virgin IV, H.W., Kyei, G.B., Johansen, T., and Vergne, I. (2010). Delivery of cytosolic components by autophagic adaptor protein p62 endows autophagosomes with unique antimicrobial properties. Immunity *32*, 329-341.
Prajsnar, T.K., Serba, J.J., Dekker, B.M., Gibson, J.F., Masud, S., Fleming, A., Johnston, S.A., Renshaw, S.A., and Meijer, A.H. (2021). The autophagic response to Staphylococcus aureus provides an intracellular niche in neutrophils. Autophagy *17*, 888-902.

Rougeot, J., Torraca, V., Zakrzewska, A., Kanwal, Z., Jansen, H.J., Sommer, F., Spaink, H.P., and Meijer, A.H. (2019). RNAseq profiling of leukocyte populations in zebrafish larvae reveals a cxcl11 chemokine gene as a marker of macrophage polarization during mycobacterial infection. Frontiers in immunology *10*, 832.
Sanjuan, M.A., Dillon, C.P., Tait, S.W., Moshiach, S., Dorsey, F., Connell, S., Komatsu, M., Tanaka, K., Cleveland, J.L., and Withoff, S. (2007). Toll-like receptor signalling in macrophages links the autophagy pathway to phagocytosis. Nature *450*, 1253-1257.
Stamm, L.M., Morisaki, J.H., Gao, L.-Y., Jeng, R.L., McDonald, K.L., Roth, R., Takeshita, S., Heuser, J., Welch, M.D., and Brown, E.J. (2003). Mycobacterium marinum escapes from phagosomes and is propelled by actin-based motility. The Journal of experimental medicine *198*, 1361-1368.
Stockhammer, O.W., Rauwerda, H., Wittink, F.R., Breit, T.M., Meijer, A.H., and Spaink, H.P. (2010). Transcriptome analysis of Traf6 function in the innate immune response of zebrafish embryos. Molecular immunology *48*, 179-190.
Upadhyay, S., and Philips, J.A. (2019). LC3-associated phagocytosis: host defense and microbial response. Current opinion in immunology *60*, 81-90.
Van Der Sar, A.M., Musters, R.J., Van Eeden, F.J., Appelmelk, B.J., Vandenbroucke-Grauls, C.M., and Bitter, W. (2003). Zebrafish embryos as a model host for the real time analysis of Salmonella typhimurium infections. Cellular microbiology *5*, 601-611.
van der Vaart, M., Banducci-Karp, A., Forn-Cuní, G., Witt, P.M., Willemse, J.J., Sánchez, S.M., Hosseini, R., and Meijer, A.H. (2020). DRAM1 requires PI (3, 5) P2 generation by PIKfyve to deliver vesicles and their cargo to endolysosomes. bioRxiv.
van der Vaart, M., Korbee, C.J., Lamers, G.E., Tengeler, A.C., Hosseini, R., Haks, M.C., Ottenhoff, T.H., Spaink, H.P., and Meijer, A.H. (2014). The DNA damage-regulated autophagy modulator DRAM1 links mycobacterial recognition via TLR-MYD88 to autophagic defense. Cell host & microbe *15*, 753-767.
Xie, Y., Xie, J., Meijer, A.H., and Schaaf, M.J. (2021). Glucocorticoid-induced exacerbation of mycobacterial infection is associated with a reduced phagocytic capacity of macrophages. Frontiers in immunology *12*, 618569.
Xu, Y., Zhou, P., Cheng, S., Lu, Q., Nowak, K., Hopp, A.-K., Li, L., Shi, X., Zhou, Z., and Gao, W. (2019). A bacterial effector reveals the V-ATPase-ATG16L1 axis that initiates xenophagy. Cell *178*, 552-566. e520.
Zhang, R., Varela, M., Forn-Cuní, G., Torraca, V., van der Vaart, M., and Meijer, A.H. (2020). Deficiency in the autophagy modulator Dram1 exacerbates pyroptotic cell death of Mycobacteria-infected macrophages. Cell death & disease *11*, 1-16.
Zhang, X.-D., Qi, L., Wu, J.-C., and Qin, Z.-H. (2013). DRAM1 regulates autophagy flux through lysosomes. PLoS one *8*, e63245.

## Supplementary figures

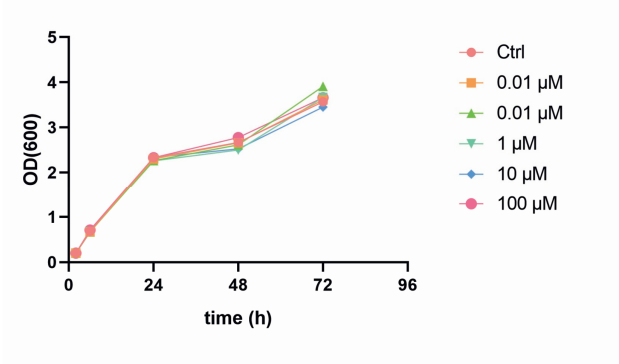


**Figure S1**. **TIPTP does not affect the growth of *S.* Typhimurium.** The OD600 of *S.* Typhimurium cultures with the indicated concentrations of TIPTP was measured over a time course of 72h.

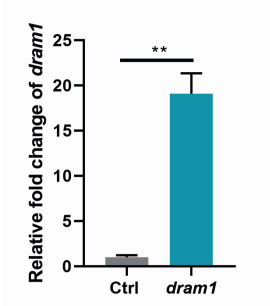


**Figure S2. Confirmation of *dram1* overexpression in zebrafish after *dram1* mRNA injection.** qPCR analysis of *dram1* expression levels in control and overexpression groups at 2dpi. *dram1* expression levels relative to the control and normalized to *tbp* are indicated. (**p<0.001).

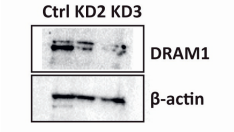


**Figure S3. Confirmation of DRAM1 knockdown in D*ram1* knockdown RAW 264.7 macrophages.** Western blot analysis of DRAM1 protein levels in control and knockdown cells. DRAM1 protein levels quantified relative to the control and normalized to beta-actin are indicated.

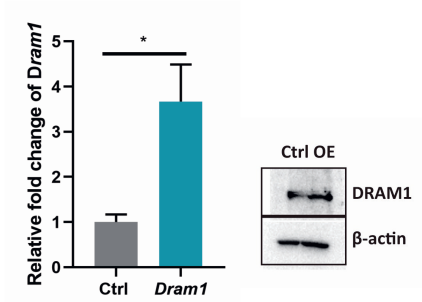


**Figure S4. Confirmation of DRAM1 overexpression in D*ram1* overexpressing RAW 264.7 macrophages. (A)** qPCR analysis of *Dram1* expression levels in control and *Dram1* overexpressing cell lines. *Dram1* expression levels relative to the control and normalized to *Gapdh* are indicated. (*p<0.05). **(B)** Western blot analysis of DRAM1 protein levels in control and overexpression cells. DRAM1 protein levels quantified relative to the control and normalized to beta-actin are indicated.

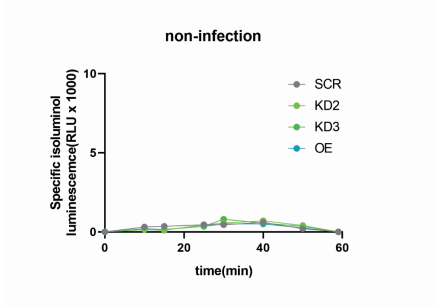


**Figure S5: Isoluminol measurement of ROS production in non-infected *Dram1* knockdown, overexpression and control RAW 264.7 macrophages.** Graphs show the data from one replicate out of two independent experiments. Lack of statistical differences was demonstrated by one-way ANOVA and pairwise comparison with Dunnett correction.